Journal of Biomolecular NMR, 10 (1997) 29–43

J-Bio NMR 442

Solution conformation and dynamics of a tetrasaccharide related to the Lewis^X antigen deduced by NMR relaxation measurements

Ana Poveda[a], Juan Luis Asensio[b], Manuel Martín-Pastor[b] and Jesús Jiménez-Barbero[b,*]

[a]*Servicio Interdepartamental de Investigación, Universidad Autónoma de Madrid, Cantoblanco, E-28049 Madrid, Spain*
[b]*Grupo de Carbohidratos, Instituto de Química Orgánica, CSIC, Juan de la Cierva 3, E-28006 Madrid, Spain*

Received 7 January 1997
Accepted 4 March 1997

Keywords: Relaxation; Dynamics; Oligosaccharide; Model-free approach; Internal motion

Summary

^{1}H-NMR cross-relaxation rates and nonselective longitudinal relaxation times have been obtained at two magnetic fields (7.0 and 11.8 T) and at a variety of temperatures for the branched tetrasaccharide methyl 3-*O*-α-*N*-acetyl-galactosaminyl-β-galactopyranosyl-(1→4)[3-*O*-α-fucosyl]-glucopyranoside (**1**), an inhibitor of astrocyte growth. In addition, ^{13}C-NMR relaxation data have also been recorded at both fields. The ^{1}H-NMR relaxation data have been interpreted using different motional models to obtain proton–proton correlation times. The results indicate that the GalNAc and Fuc rings display more extensive local motion than the two inner Glc and Gal moieties, since those present significantly shorter local correlation times. The ^{13}C-NMR relaxation parameters have been interpreted in terms of the Lipari–Szabo model-free approach. Thus, order parameters and internal motion correlation times have been deduced. As obtained for the ^{1}H-NMR relaxation data, the two outer residues possess smaller order parameters than the two inner rings. Internal correlation times are in the order of 100 ps. The hydroxymethyl groups have also different behaviour, with the exocyclic carbon on the glucopyranoside unit showing the highest S^2. Molecular dynamics simulations using a solvated system have also been performed and internal motion correlation functions have been deduced from these calculations. Order parameters and interproton distances have been compared to those inferred from the NMR measurements. The obtained results are in fair agreement with the experimental data.

Introduction

Oligosaccharides are involved in a variety of recognition events as cell adhesion, metastasis and embryonic development, among others (Bundle and Young, 1992; Lasky, 1992). To play a role in these functions, the 3D structure of the carbohydrate is of primary importance (Bock, 1983; Homans, 1990; Bush, 1992; De Waard et al., 1992; Homans and Forster, 1992; Peters et al., 1993; Rice et al., 1993; Rutherford and Homans, 1994; Van Halbeek, 1994; Rutherford et al., 1995). The extent and nature of the motion around the glycosidic linkages of oligosaccharides remains an open question (Hricovini et al., 1992; Hajduk et al., 1993; Rutherford et al., 1993; Hardy et al., 1995; Hricovini and Torri, 1995) and even detailed analyses of results have concluded either constrained conformations (Lemieux et al., 1980; Lemieux, 1989) or conformational averaging (Edge et al., 1990; Leeflang and Kroon-Batenburg, 1992; Carver, 1993; Peters and Weimar, 1994; Poveda et al., 1996) for different, or even the same, carbohydrate structures. At present, it is obvious that complete rigidity may be discarded. However, the ways of looking at the concept of flexibility are quite subjective and may range from the consideration of small

*To whom correspondence should be addressed.
Dedicated to Prof. Dr. Manuel Rico on the occasion of his 60th birthday.
Abbreviations: GalNAc, *N*-acetyl galactosamine; Gal, galactose; Glc, glucose; Fuc, fucose.

TABLE 1
RELEVANT INTRA- AND INTERRESIDUE PROTON–PROTON AVERAGE CORRELATION TIMES ESTIMATED AT FOUR DIFFERENT TEMPERATURES FROM $\sigma_{NOE}^{500\ MHz}/\sigma_{ROE}^{500\ MHz}$, $\sigma_{NOE}^{300\ MHz}/\sigma_{ROE}^{300\ MHz}$, $\sigma_{NOE}^{500\ MHz}/\sigma_{NOE}^{300\ MHz}$ RATIOS

Proton pair	Correlation time (ns) at temperature			
	299 K	302 K	313 K	320 K
Fuc H-1/H-2	0.71	0.64	0.48	0.31
Fuc H-1/Glc H-3	0.71	0.64	0.48	0.31
Fuc H-1/Glc H-2	0.71	0.63	0.39	0.32
GalNAc H-1/H-2	0.80	0.70	0.51	0.39
GalNAc H-1/Gal H-4	0.76	0.59	0.46	0.36
GalNAc H-1/Gal H-3	0.74	0.63	0.43	0.36
Gal H-1/Glc H-4	0.89	0.79	0.53	Overlap H_2O
Gal H-1/H-3	**0.96**	**0.86**	0.57	Overlap H_2O
Gal H-1/Glc H-6a	0.77	0.65	0.48	Overlap H_2O
Gal H-1/H-5	0.86	0.79	0.55	Overlap H_2O
Glc H-1/H-3	0.86	0.79	0.59	**0.47**
Glc H-1/H-5	0.90	0.76	**0.61**	0.37
Fuc H-5/H-3	0.73	0.57	0.39	0.27
Fuc H-5/H-4	0.70	0.58	0.43	0.33
Fuc H-5/CH_3-6	0.68	0.52	0.39	0.25
Fuc H-5/Gal H-2	0.74	0.58	0.44	0.32
Fuc CH_3-6/Gal H-2	0.54	0.53	0.32	0.24
Fuc CH_3-6/Fuc H-4	0.50	0.57	0.32	0.25

The highest correlation time at a given temperature is indicated in bold. Estimated errors are better than 15%.

torsional oscillations around a given conformer to the recognition of the simultaneous presence of two or more significantly different geometries (Dabrowski et al., 1995). An indication of internal motion around glycosidic linkages has been directly obtained in small sugars as sucrose (Poppe and Van Halbeek, 1992; Engelsen et al., 1995; Maler et al., 1996b), and other small and medium-sized saccharides for which, in addition, recent investigations have indicated that the rates of overall and internal motions (Abseher et al., 1994; Philippopoulos and Lim, 1994) may occur on similar timescales (Hricovini et al., 1992; Braccini et al., 1993; Hajduk et al. 1993; Meyer et al., 1993; Rutherford et al., 1993; Hardy et al., 1995; Hricovini and Torri, 1995). Recent evidence of the existence of flexibility in branched oligosaccharides has also been reported (Lommerse et al., 1995; Maler et al., 1996a). The existence of rigid or flexible structures is of prime importance in recognition phenomena, since any bimolecular binding process is entropically unfavourable (Searle and Williams, 1992).

The conformation of the Le^X determinant and analogues has been the subject of intensive research during the past few years due to their implication in inflammatory processes (Ball et al., 1992; Ichikawa et al., 1992; Mukhopadhyay et al., 1994; Rutherford et al., 1994). The reported results indicate that, in all the studied compounds, the branched Le^X trisaccharide moiety, Galβ-(1→4)[Fucα(1→3)]GlcNAc, is rather rigid. It has recently been reported that an Le^X-related compound, namely GalNAcα(1→3)Galβ(1→4)[Fucα(1→3)]GlcβOMe (**1**), shows inhibitory activity against the proliferation of astrocytes and transformed neural cell lines (Santos-Benito et al., 1992). In addition, a variety of analogues were synthesized that showed different inhibitory potencies (Singh et al., 1994; Coteron et al., 1995).

We now report on the application of both homo- and heteronuclear NMR relaxation measurements, measured at different temperatures and magnetic fields, assisted by molecular dynamics simulations, to unequivocally characterize that, in contrast to common belief, an Le^X tetrasaccharide analogue, **1**, presents differential conformational flexibility for the several glycosidic linkages in solution.

Methods

Molecular dynamics

Molecular mechanics and dynamics calculations were performed using the CVFF force field within the INSIGHTII/DISCOVER (Hagler et al., 1979) programs of Biosym Technologies (San Diego, CA, U.S.A.). Two independent molecular dynamics simulations were carried out. The initial structure (Coteron et al., 1995) was extensively minimized and then solvated with 545 water molecules in a cubic box of 26 Å, giving a density of ca. 1 g cm^{-3}. A cutoff of 11 Å was used for nonbonding interactions. Periodic boundary conditions and the minimum image model were employed. The simulations were performed at 310 K with a 1 fs integration step. The equilibration period was 15 ps. After this period, structures were saved every 15 fs. This short saving frequency was essential to get good correlation functions. In total, about

14 000 structures were collected for every simulation. An in vacuo 1 ns simulation was also acquired. Molecular dynamics trajectories were analysed using software written at home. Overall reorientation was removed by diagonalizing the inertia tensor and subsequent superimposition of the principal inertia axis of every frame (Bruschweiler et al., 1992). Then, internal correlation functions were calculated, and, from these functions, generalized order parameters and internal correlation times were deduced, according to the Lipari and Szabo (1982) model-free approach. In addition, average distances between intraresidue and interresidue proton pairs were calculated from the dynamics simulations.

NMR experiments

NMR experiments were recorded on Varian Unity 500 and Bruker AMX-300 spectrometers, using 5 mM (^{1}H-NMR) and 10 mM (^{13}C-NMR) solutions of **1** in 3:1 D_2O:DMSO-d_6. This solvent mixture was chosen in order to increase the global correlation time of the molecule and to get negative NOEs at room temperature even at 300 MHz. NOESY experiments (Neuhaus and Williamson, 1989) were recorded using mixing times of 100, 200, 400, 600 and 800 ms. ROESY experiments (Bothner-By et al., 1984) used mixing times of 100, 200, 300 and 400 ms. The rf carrier frequency was set at δ 6.0 ppm, and the spin locking field was 2.5 kHz. The experiments were carried out at 299, 302, 313, 320 and 333 K. Standard temperature control was used. Cross-relaxation rates were obtained as described (Poppe and Van Halbeek, 1992) from the corresponding build up curves by extrapolation at zero mixing time. ^{1}H-NMR longitudinal nonselective relaxation times were obtained using the standard inversion recovery method (Neuhaus and Williamson, 1989) by a nonlinear three-parameter fit of peak intensities.

In a first step, assuming the spectral density functions of models I–IV (see below), correlation times (Table 1) were estimated from σ ratios, by solving the resultant quartic equation, which exclusively depends on the correlation time of the corresponding proton pair and on the spectrometer frequency.

$$\sigma_{NOESY}/\sigma_{ROESY} = (5 + 22\,\omega_0^2\,\tau_c^2 + 8\,\omega_0^4\,\tau_c^4)/(5 + \omega_0^2\,\tau_c^2 - 4\,\omega_0{}^2\,\tau_c^4) \quad (1)$$

Next, different motional models were used to correlate the experimental ^{1}H-NMR measurements with the molecular dynamics results and to extract order parameters, S^2 (or S_f^2) and overall, τ_0, and internal motion, τ_e (or effective, τ_{eff}), correlation times for the different atom pairs of the tetrasaccharide. In this work, we considered the Lipari and Szabo (1982) model-free approach (for both proton and carbon data) and different approximations thereof, as described by Lommerse et al. (1995). These approximations are:

Model I: Rigid isotropic motion, with only one global correlation time (Eq. 2).

$$J(\omega) = \frac{\tau_0}{1 + (\omega\tau_0)^2} \quad (2)$$

Model II (Eq. 3): The spectral density function is modified by assuming different generalized order parameters (S_f^2) for every proton–proton pair. Thus, the global correlation time accounts for the slow motions of the molecule and S_f^2 for the fast internal motions around the glycosidic linkages and/or the monosaccharide rings (first term of the spectral density function within the model-free approach).

$$J(\omega) = S_f^2\,\frac{\tau_0}{1 + (\omega\tau_0)^2} \quad (3)$$

Model III: If the S_f^2 order parameters are not available, it is possible to include fast internal motions by assuming different effective correlation times for every proton pair (Eq. 4).

$$J(\omega) = \frac{\tau_{eff}}{1 + (\omega\tau_{eff})^2} \quad (4)$$

Model IV: Both S_f^2 and effective correlation times are used for every proton pair (Eq. 5).

$$J(\omega) = S_f^2\,\frac{\tau_{eff}}{1 + (\omega\tau_{eff})^2} \quad (5)$$

Model V: The regular Lipari–Szabo model-free approach, where τ_e represents a single effective correlation time describing the internal motions (Eq. 6).

$$J(\omega) = \frac{S^2\tau_0}{(1 + \omega^2\tau_0^2)} + \frac{(1 - S^2)\tau}{(1 + \omega^2\tau^2)} \quad (6)$$

where $\tau = \tau_0\tau_e/(\tau_0 + \tau_e)$.

A simplex algorithm was used for fitting the experimental data to the different models (Craik et al., 1983). A target function R_w was defined (Eq. 7), which represents the deviation between the calculated relaxation data and the experimental, with $R_w = 0$ for an exact fit.

$$R_w = \sqrt{\sum_{i=1}^{n} \frac{(\sigma_{NOE_i}^{calc} - \sigma_{NOE_i}^{exp})^2 + (\sigma_{ROE_i}^{calc} - \sigma_{ROE_i}^{exp})^2 + (\sigma_{T\text{-}ROE_i}^{calc} - \sigma_{T\text{-}ROE_i}^{exp})^2}{(\sigma_{NOE_i}^{exp})^2 + (\sigma_{ROE_i}^{exp})^2 + (\sigma_{T\text{-}ROE_i}^{exp})^2}} \quad (7)$$

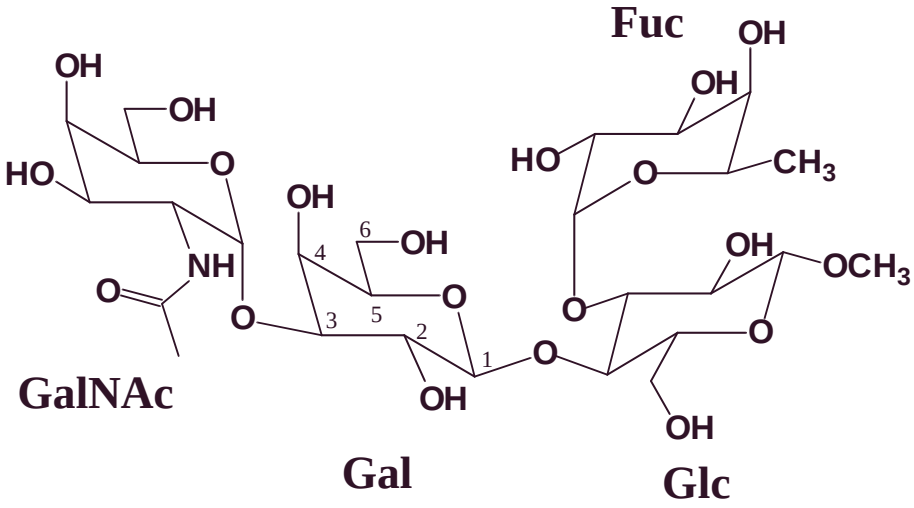

Fig. 1. Schematic view of tetrasaccharide **1**, showing the atomic numbering.

The subscript i represents data for a particular proton pair, and n is the total number of proton pairs with available experimental data.

The fit to the experimental data at 299 K was done in independent runs, for the intraresidue proton pairs (since there are basically no errors in their corresponding average distances) and, then, for the interresidue proton pairs. Two cases were considered. In the first case, experimental intraresidue cross-relaxation rates (from both 300 and 500 MHz NOESY and ROESY experiments) were used as input, along with the average distances and order parameters, deduced from the solvated MD simulations (Bruschweiler et al., 1992). The program then iteratively calculated the effective (or overall, depending on the model) correlation times which produced the best fit to the experimental data, depending on the chosen motional model. Then, for the interresidue proton pairs, the fastest local correlation time of the two pyranoid rings involved in the glycosidic linkage was chosen (Lommerse et al., 1995) and the goodness of the fit evaluated.

In the second case, only the MD-derived distances were used as input, along with the intraresidue cross-relaxation rates. This approximation is more general and no accurate order parameters are necessary, provided that enough experimental data are available. Since, in this case, both transversal and longitudinal cross-relaxation rates at two different magnetic fields are available, the program is able to estimate the effective (or overall, depending on the model) correlation times and S^2 (or S_f^2) which produced the smallest R_w, by using a simplex-based algorithm. Calculations for the intra- and interresidue proton pairs were also separated. In addition, different runs, using either all the relaxation parameters or leaving just one set (NOESY300, NOESY500, ROESY300, ROESY500) of cross-relaxation rates, were performed. In these cases, the parameter not used in the adjustment was employed as a test of the goodness of the fitting approach, by a comparison of the simulated experimental data (using the optimized motional parameters) with the experimental ones. Finally, in order to get an indication of the internal consistency of the results, intraresidue distances were back-calculated from the deduced motion parameters and experimental cross-relaxation rates.

^{13}C-NMR T_1 relaxation times were obtained by both the regular 1D carbon detection inversion recovery and the 2D double INEPT based inverse detection methods (Barbato et al., 1992) at 26 °C at both 7 and 11.8 T, by using a nonlinear three-parameter fit of peak intensities. The errors are estimated to be less than 10%. At least seven different relaxation delays were used in every experiment with a repetition delay of 4 s. Transverse T_2 relaxation times were measured by using the sequence proposed by Kay et al. (1992). All the given values are averaged among the different measurements performed. NOEs were obtained by using the standard carbon-detected 1D protocol with a repetition delay of 4 s. The accuracy in the NOE factor is estimated to be smaller than 0.1. ^{13}C-NMR relaxation parameters were interpreted according to the previously mentioned model-free approach (Lipari and Szabo, 1982) and the other approximations by a least-squares fitting procedure.

A similar target function, R_w, was also defined, Eq. 8:

$$R_w = \sqrt{\sum_{i=1}^{n} \frac{(T_{1_i}^{calc} - T_{1_i}^{exp})^2 + (T_{2_i}^{calc} - T_{2_i}^{exp})^2 + (NOE_i^{calc} - NOE_i^{exp})^2}{(T_{1_i}^{exp})^2 + (T_{2_i}^{exp})^2 + (NOE_i^{exp})^2}} \quad (8)$$

with $R_w = 0$ for an exact fit. The subscript i represents data for a particular carbon atom, and n is the total number of carbons with available experimental data.

As stated above, either all the relaxation parameters or combinations of two of them (always at both magnetic fields) were used. The parameter which was not taken into account in the fitting procedure was employed as a test of the goodness of the fitting approach. In all cases, for the different models, only the results of the best fitting (smallest R_w), that include all the experimental data, are given in the text.

Results and Discussion

^{1}H-NMR relaxation measurements

The experiments were carried out in a 1:3 DMSO:D_2O mixture in order to increase the overall correlation time of the molecule and to enter into the negative NOE regime at room temperature. It is thus expected that the difference between overall and internal motion fast correlation times is increased. It is well known that 25% of DMSO in water does not modify the conformational features of oligosaccharides (Yan et al., 1987). In addition, only minor differences in the proton chemical shifts (<0.05 ppm) of the oligosaccharide were observed when passing from pure D_2O to the DMSO:D_2O mixture. The pyranoid rings can be described as essentially monoconformational: the Glc, Gal and GalNAc rings are $^4C_1$ and the Fuc is $^1C_4$, as deduced from the vicinal proton–proton couplings. Intra- and interresidue NOEs were obtained for the tetrasaccharide **1** (Fig. 1) through 2D NOESY and 2D ROESY experiments at five different temperatures (between 299 and 323 K) and at two different magnetic fields (300 and 500 MHz). Cross-relaxation rates (σ_{ROE},σ_{NOE}) were obtained from these measurements (Poppe and Van Halbeek, 1992). A first attempt to characterize the presence of internal motion was performed by obtaining $\sigma_{ROE}/\sigma_{NOE}$ ratios (Davis, 1987; Bruschweiler et al., 1992; Abseher et al., 1994; Philippopoulos and Lim, 1994) at two magnetic fields (Hricovini et al., 1992), since they allow one to estimate specific correlation times (Table 1). There are small, but significant, differences between these ratios. In all cases and at all the temperatures studied, it can be observed that the obtained correlation times for proton pairs belonging to either the Gal or the Glc residues are higher than those within the Fuc and GalNAc rings. Direct experimental evidence of differential flexibility for the GalNAc and Fuc residues of **1** was obtained by a visual inspection of the cross-peak signs at the different temperatures. We will comment on the results at 300 MHz. Indeed, although in the NOESY spectra at 299 K NOE effects for all the residues were negative, NOESY cross peaks for the Fuc residue at 302 K were positive, those for Glc, Gal and GalNAc being still negative or zero. In addition, and at 313 K, cross peaks for both Fuc and GalNAc were clearly positive, while those for Gal and Glc were approximately zero. Therefore, according to the experimental results and unexpectedly, the glycosidic linkage for the Fuc residue at the branching Glc moiety is as flexible or even more flexible than that for the terminal GalNAc ring. The observed results at 500 MHz are similar but the temperature required for observing differential signs is higher, ca. 318 K. A check of the internal consistency of the results was performed by back-calculating the intraresidue proton/proton distances at the different temperatures (Table 2). It can be observed that there is a fair agreement between experimental and modelled distances. Based on the good matching for these intraresidue distances, experimental interresidue distances were also calculated and

TABLE 2
MD $\langle r^{-6}\rangle^{-1/6}$ AVERAGE DISTANCES AND THOSE CALCULATED FROM THE AVERAGE CORRELATION TIMES OBTAINED FROM $\sigma_{NOE}^{500\ MHZ}/\sigma_{ROE}^{500\ MHZ}$, $\sigma_{NOE}^{300\ MHZ}/\sigma_{ROE}^{300\ MHZ}$, $\sigma_{NOE}^{500\ MHZ}/\sigma_{NOE}^{300\ MHZ}$ RATIOS AT EVERY TEMPERATURE

Proton pair	MD $\langle r^{-6}\rangle^{-1/6}$ (Å)	299 K (Å)	302 K (Å)	313 K (Å)	320 K (Å)
Intraresidue					
GalNAc H-1/H-2	2.36	2.44	2.46	2.43	2.45
Gal H-1/H-3	2.69	2.56	2.62	2.48	
Gal H-1/H-5	2.51	2.35	2.38	2.41	
Glc H-1/H-3	2.65	2.57	2.65	2.55	2.65
Glc H-1/H-5	2.51	2.36	2.30	2.23	2.26
Fuc H-1/H-2	2.34	2.52	2.53	2.53	2.65
Fuc H-5/H-4	2.43	2.35	2.38	2.35	2.30
Fuc H-5/H-3	2.54	2.57	2.61	2.57	2.61
Interresidue					
GalNAc H-1/Gal H-4	2.51	2.51	2.55	2.59	2.48
GalNAc H-1/Gal H-3	2.42	2.61	2.66	2.53	2.33
Gal H-1/Glc H-4	2.49	2.21	2.23	2.19	
Fuc H-1/Glc H-3	2.54	2.52	2.53	2.53	2.65
Fuc H-1/Glc H-2	3.59	3.28	3.27	3.41	3.21
Fuc H-5/Gal H-2	2.56	2.64	2.69	2.70	2.72

TABLE 3
RATIO OF THE LONGITUDINAL NONSELECTIVE RELAXATION TIMES AT TWO MAGNETIC FIELDS (500 MHz/300 MHz) FOR DIFFERENT PROTONS OF THE BRANCHED TETRASACCHARIDE

Proton	Temperature (K)				
	299	302	313	320	333
Fuc H-1	2.35	2.03	1.92	1.86	1.74
GalNAc H-1	2.32	2.10	1.94	1.94	1.93
Gal H-1	2.53	**2.27**	**2.24**	Overlap	**2.48**
Glc H-1	**2.65**	2.17	2.15	**2.12**	Overlap
Fuc H-5	1.80	1.87	1.86	1.82	1.79
Fuc CH_3-6	1.62	1.72	1.85	1.57	1.64
GalNAc H-2	2.24	2.04	1.88	1.88	1.87

The higher the ratio (in bold), the higher the restriction to internal motion. Several independent measurements were performed. The estimated error is smaller than 10%.

then compared to those derived from the solvated MD simulations, indicating that a satisfactory agreement was found between both sets of values (see the section Molecular dynamics simulations). Therefore, and according to the results indicated above, it seems that this method is robust and can provide at least a semiquantitative evaluation of motional parameters and interresidue proton/proton distances for oligosaccharide molecules.

In addition, when the ratios of nonselective longitudinal relaxation times (T_1) at different magnetic fields were calculated, it could be observed that, at all the temperatures studied, the T_1 ratios (Hricovini et al., 1992; Van Halbeek and Poppe, 1992) for the internal Gal and Glc residues were significantly larger than the T_1 ratios of the external GalNAc and Fuc residues (Table 3). Therefore, both the T_1 ratios and the existence of opposite signs for cross peaks belonging to different residues, within the same NOESY spectrum, unequivocally indicate that, even in a branched tetrasaccharide, there is a substantial amount of conformational freedom, as well as distinct flexibility for the different glycosidic linkages.

Following with the homonuclear relaxation data, a somehow more quantitative approach was performed, following a protocol similar to that described by Lommerse et al. (1995) (see also the Methods section). In this case, effective correlation times for specific proton pairs were calculated from the simultaneous evaluation of all (longitudinal and transversal) proton–proton relax-

TABLE 4
AVERAGE MOTIONAL PARAMETERS FOR DIFFERENT INTRARESIDUE PROTON PAIRS OF THE DIFFERENT MONOSACCHARIDE UNITS OF THE TETRASACCHARIDE OBTAINED AT 299 K FROM LEAST-SQUARES FITTING

Residue	Model	τ_m (ps)	S^2	τ_{eff} (ps)	R_w
Glc	I	646 ± 22	–	–	0.398
	II	841 ± 38	0.89	–	0.254
	III	–	–	914 ± 23	0.222
	IV	–	0.89	1030 ± 28	0.202
	V	1042 ± 38	0.89	30 ± 10	0.213
Gal	I	646 ± 22	–	–	
	II	841 ± 38	0.94	–	
	III	–	–	1214 ± 32	
	IV	–	0.94	1316 ± 29	
	V	1042 ± 38	0.94	39 ± 3	
Fuc	I	646 ± 22	–	–	
	II	841 ± 38	0.80	–	
	III	–	–	613 ± 12	
	IV	–	0.80	678 ± 20	
	V	1042 ± 38	0.80	50 ± 13	
GalNAc	I	646 ± 22	–	–	
	II	841 ± 38	0.81	–	
	III	–	–	624 ± 11	
	IV	–	0.81	777 ± 21	
	V	1042 ± 38	0.81	62 ± 11	

Order parameters (S^2) have been deduced from molecular dynamics simulation (see the MD section) using explicit water molecules. The proton pairs used for the fitting were Glc H-1/H-3, Glc H-1/H-5, Gal H-1/H-3, Gal H-1/H-5, GalNAc H-1/H-2, Fuc H-1/H-2, Fuc H-3/H-5 and Fuc H-4/H-5. The fitting of the interresidue data to these parameters provided R_w values of 0.493, 0.458, 0.435, 0.396 and 0.390, respectively.

TABLE 5
AVERAGE MOTIONAL PARAMETERS FOR DIFFERENT INTRARESIDUE PROTON PAIRS OF THE DIFFERENT MONOSACCHARIDE UNITS OF THE TETRASACCHARIDE OBTAINED AT 299 K FROM LEAST-SQUARES FITTING

Residue	Model	τ_m (ps)	S^2	τ_{eff} (ps)	R_w
Glc	I	771 ± 10	–	–	0.358
	II	1225 ± 18	0.90	–	0.324
	III	–	–	1193 ± 13	0.192
	IV	–	1.00	1193 ± 13	0.195
	V	1299 ± 28	0.85	36 ± 16	0.190
Gal	I	771 ± 10	–	–	
	II	1225 ± 18	1.00	–	
	III	–	–	1414 ± 22	
	IV	–	1.00	1414 ± 22	
	V	1299 ± 28	0.99	34 ± 5	
Fuc	I	771 ± 10	–	–	
	II	1225 ± 18	0.60	–	
	III	–	–	719 ± 22	
	IV	–	0.83	838 ± 30	
	V	1299 ± 28	0.53	86 ± 12	
GalNAc	I	771 ± 10	–	–	
	II	1225 ± 18	0.61	–	
	III	–	–	624 ± 11	
	IV	–	0.75	777 ± 21	
	V	1299 ± 28	0.51	72 ± 30	

Order parameters (S^2) have also been deduced from the fitting procedure. The proton pairs used for the fitting were Glc H-1/H-3, Glc H-1/H-5, Gal H-1/H-3, Gal H-1/H-5, GalNAc H-1/H-2, Fuc H-1/H-2, Fuc H-3/H-5 and Fuc H-4/H-5. The fitting of the interresidue data to these parameters provided R_w values of 0.444, 0.416, 0.406, 0.410 and 0.400, respectively.

ation rates deduced at 299 K. Average interproton distances (from $\langle r^{-3}\rangle^{-1/3}$) were obtained from MD simulations (see below) and employed in the study. Order parameters were estimated from internal motion correlation functions, also calculated from MD trajectories (see below and the experimental section). A fit of the experimental NOE and ROE data to those calculated for different simplifications of the model-free approach described by Lipari and Szabo (1982) allowed one to have estimations of the local and/or global correlation times. Intraresidue proton pairs were first evaluated, since they are basically independent of the conformation around the glycosidic linkages. The goodness of the fit was evaluated by using a residual factor (Gonzalez et al., 1991).

TABLE 6
MD AVERAGE DISTANCES AND AVERAGE BACK-CALCULATED DISTANCES FOR MODELS I–V AT 299 K, USING THE MOTIONAL PARAMETERS OBTAINED FROM THE LEAST-SQUARES FITTING OF THE INTRARESIDUE CROSS-RELAXATION RATES DATA

Proton pair	MD $\langle r^{-6}\rangle^{-1/6}$–$\langle r^{-3}\rangle^{-1/3}$ (Å)	Model I (Å)	Model II (Å)	Model III (Å)	Model IV (Å)	Model V (Å)
Intraresidue						
Gal H-1/H-3	2.69–2.70	2.48	2.76	2.87	2.87	2.77
Gal H-1/H-5	2.51–2.52	2.36	2.62	2.65	2.65	2.63
GalNAc H-1/H-2	2.36–2.36	2.42	2.46	2.17	2.36	2.46
Glc H-1/H-3	2.65–2.66	2.58	2.76	2.69	2.69	2.70
Glc H-1/H-5	2.51–2.52	2.34	2.59	2.68	2.68	2.60
FucH-1/H-2	2.34–2.35	2.73	2.71	2.49	2.37	2.71
Fuc H-5/H-4	2.43–2.43	2.52	2.65	2.53	2.53	2.54
Fuc H-5/H-3	2.54–2.55	2.69	2.72	2.40	2.57	2.59
Interresidue						
Gal H-1/Glc H-4	2.49–2.50	2.13	2.46	2.65	2.65	2.48
GalNAc H-1/Gal H-3	2.42–2.46	2.56	2.77	2.59	2.59	2.62
GalNAc H-1/Gal H-4	2.51–2.58	2.58	2.68	2.35	2.62	2.64
Fuc H-1/Glc H-2	3.59–3.60	3.43	3.99	3.92	3.92	3.95
Fuc H-1/Glc H-3	2.54–2.56	2.64	2.86	2.65	2.65	2.68
Fuc H-5/Gal H-2	2.56–2.61	2.59	2.68	2.32	2.63	2.67

TABLE 7
RELAXATION PARAMETERS OF THE CARBON SIGNALS FOR THE TETRASACCHARIDE, OBTAINED AT TWO MAGNETIC FIELDS AT 299 K; THE AVERAGE VALUES FOR EACH RING ARE ALSO GIVEN

Carbon atom	T_1 (ms)		NOE		T_2 (ms)	
	7.1 T	11.8 T	7.1 T	11.8 T	7.1 T	11.8 T
Glc-1	162	268	1.58	1.34	150	201
Glc-2	136	247	1.72	1.37	131	173
Glc-3	146	238	1.58	1.31	121	142
Glc-4	137	227	1.63	1.43	132	174
Glc-5	152	231	1.62	1.33	141	182
Average	147	242	1.63	1.36	135	174
Gal-1	162	246	1.45	1.40	151	192
Gal-2	153	240	1.58	1.40	133	164
Gal-3	121	226	1.63	1.27	122	141
Gal-4	145	224	1.58	1.33	133	145
Gal-5	152	247	1.69	1.35	131	183
Average	147	237	1.59	1.35	134	165
Fuc-1	171	269	1.61	1.41	169	236
Fuc-2	155	256	1.74	1.46	157	208
Fuc-3	161	250	1.69	1.35	157	169
Fuc-4	171	272	1.63	1.38	148	207
Fuc-5	152	242	1.65	1.56	149	205
Average	162	258	1.66	1.43	156	205
GalNAc-1	160	261	1.66	1.45	168	208
GalNAc-2	158	225	1.64	1.38	151	174
GalNAc-3	156	274	1.67	1.39	146	159
GalNAc-4	160	256	1.74	1.46	147	183
GalNAc-5	148	257	1.62	1.40	143	196
Average	156	244	1.67	1.42	151	184
Glc-6	140	147	1.60	1.51	81	91
Gal-6	–	163	2.11	1.85	100	121
Fuc-6	321	425	2.33	2.32	251	260
GalNAc-6	150	190	2.46	2.25	119	136

Estimated errors are smaller than 10%.

Two facts are evident from this analysis (Table 4). In all cases, the residual factor, R_w, decreases with increasing complexity of the spectral density function, thus indicating that the explicit consideration of torsional flexibility around the glycosidic linkages, indeed, increases the fit between theoretical and observed data. Besides, and independently of the model employed in the calculation, the obtained local correlation times for proton pairs within the Glc or Gal rings are always higher than those belonging to the Fuc or GalNAc moieties. This fact is an indication of distinct flexibility for these two rings when compared to the lactose (Gal-β-(1→4)-Glc) moiety, as also deduced from the more qualitative analysis employed above. It is noteworthy to mention that the best fit is obtained for models III–V, which consider different motional parameters for every proton pair in the molecule. In the case of model V, internal motion correlation times around 100 ps were deduced. Finally, and in order to get an indication of the internal consistency of the method, intraresidue distances were back-calculated from the deduced motional parameters and the experimental cross-relaxation times. The obtained distances are indeed similar to those expected for chair conformations. Then, interresidue cross-relaxation rates were also evaluated, using the fastest correlation time deduced for the two protons involved (Table 4, see also the experimental section for details). Again, and as stated for the intraresidue proton pairs, the best fit (small R_w) was obtained when spectral density functions with explicit consideration of different proton–proton local correlation times (Lommerse et al., 1995) are employed (models III–V).

A more general approach was also tried, which can be useful when no accurate order parameters are available from solvated MD simulations. Using the experimental intraresidue cross-relaxation rates, all the motional parameters (correlation times and S^2) of the spectral density

functions of models I–V were optimized using a simplex-based algorithm. The R_w values are of the same order of magnitude as those deduced above when using the MD-derived order parameters. It can be observed that, for the more rigid Gal and Glc residues, similar order parameters (Table 5) to those deduced from the MD simulations were found. On the other hand, the obtained order parameters involving the Fuc and GalNAc rings were significantly shorter (about 0.2–0.3 units) than those estimated from MD. Therefore, the analysis of the experimental homonuclear data following this approach seems to point out the presence of more flexibility for the Fuc and GalNAc residues than that predicted from the simulations (see below). In this case, intraresidue distances were also back-calculated (Table 6) to get an indication of the internal consistency of the protocol, producing a satisfactory agreement with those expected for the corresponding chairs. The distances are also remarkably similar to those obtained above from σ ratios and to those derived using the order parameters derived from the MD simulations. Again, a higher degree of flexibility for the Fuc and GalNAc residues is evident from the obtained data. The degree of adjustment of the interresidue cross-relaxation rates to these motional parameters was also evaluated, thus allowing an estimation of the corresponding interresidue distances (Table 6). The agreement between the calculated (from MD, see below) and experimental interresidue distances is also fair. Therefore, it can be concluded that this protocol, combining longitudinal and transversal cross-relaxation rates, may allow one to have estimations of the internal motion timescales in oligosaccharide molecules, along with the corresponding interresidue proton/proton distances.

A recent paper on the conformation and dynamics of a trisaccharide analogue has also addressed the use of local correlation times to derive interproton distances, by simultaneous determination of the dipolar longitudinal and transversal cross-relaxation rates through off-resonance ROESY measurements (Berthault et al., 1996). These authors also concluded that, for each pair of protons, a different correlation time should be used.

^{13}C-NMR relaxation measurements

Recent studies have demonstrated the importance of the analysis of heteronuclear relaxation data to detect the presence of internal motion in biomolecules in general (Wagner, 1993), and in carbohydrates in particular (Bagley et al., 1992; Roy et al., 1993; Dais, 1994; Kowalewski and Widmalm, 1994; Poppe et al., 1994; Engelsen et al., 1995; Maler et al., 1995,1996a,b). T_1 and T_2 relaxation times and heteronuclear NOE values were obtained as described in the experimental section, at two different magnetic fields (Table 7). The data (including T_2) were satisfactorily adjusted by considering isotropic motion. According to previous reports, no major anisotropy was expected for this branched tetrasaccharide (Ejchart et al., 1992; Ejchart and Dabrowski, 1992). At both magnetic fields, the average values of NOE, T_2 and T_1 of the Fuc and GalNAc residues are larger than those of the Glc and Gal moieties. This fact is indicative of distinct flexibility of the glycosidic linkages in the different monosaccharide rings. The application of the Lipari and Szabo (1982)

TABLE 8
MOTIONAL PARAMETERS FOR THE TETRASACCHARIDE OBTAINED AT 299 K FROM LEAST-SQUARES FITTING OF RING CARBONS; THE COMPARISON WITH THE AVERAGE S^2 VALUES DEDUCED FROM MD SIMULATIONS IS ALSO GIVEN

Ring	Model	τ_m (ps)	S^2_{exp}	S^2_{MD}	τ_{eff} (ps)	R_w
Glc	I	841 ± 13	–		–	0.162
	II	846 ± 36	0.94	0.92	–	0.155
	III	–	–		1000 ± 11	0.060
	IV	–	0.91	0.92	1005 ± 12	0.043
	V	1052 ± 29	0.88	0.92	78 ± 14 (τ_{int})	0.029
Gal	I	841 ± 13	–		–	0.162
	II	846 ± 36	0.95	0.95	–	0.155
	III	–	–		1054 ± 24	0.060
	IV	–	0.92	0.95	1057 ± 17	0.043
	V	1052 ± 29	0.92	0.95	60 ± 6 (τ_{int})	0.029
Fuc	I	841 ± 13	–		–	0.162
	II	846 ± 36	0.85	0.82	–	0.155
	III	–	–		913 ± 9	0.060
	IV	–	0.83	0.82	920 ± 10	0.043
	V	1052 ± 29	0.77	0.82	90 ± 8 (τ_{int})	0.029
GalNAc	I	841 ± 13	–		–	0.162
	II	846 ± 36	0.88	0.79	–	0.155
	III	–	–		922 ± 16	0.060
	IV	–	0.86	0.79	927 ± 17	0.043
	V	1052 ± 29	0.81	0.79	94 ± 9 (τ_{int})	0.029

R_w is a measurement of the deviation between observed and calculated relaxation data.

TABLE 9
MOTIONAL PARAMETERS FOR THE METHYLENE AND METHYL GROUPS OF THE BRANCHED TETRASACCHARIDE OBTAINED AT 299 K FROM LEAST-SQUARES FITTING; THE COMPARISON WITH THE S^2 VALUES DEDUCED FROM MD SIMULATIONS IS ALSO GIVEN

Carbon	Model	τ_m (ps)	S^2_{exp}	τ_{eff} (ps)	R_w
Glc-6	I	841 ± 13	–	–	0.162
	II	846 ± 36	0.69	–	0.155
	III	–	–	937 ± 11	0.060
	IV	–	0.77	941 ± 8	0.043
	V	1052 ± 29	0.61	34 ± 4 (τ_{int})	0.029
Gal-6	I	841 ± 13	–	–	0.162
	II	846 ± 36	0.64	–	0.155
	III	–	–	509 ± 10	0.060
	IV	–	0.67	510 ± 12	0.043
	V	1052 ± 29	0.42	91 ± 5(τ_{int})	0.029
Fuc-6	I	841 ± 13	–	–	0.162
	II	846 ± 36	0.25	–	0.155
	III	–	–	309 ± 18	0.060
	IV	–	0.36	324 ± 19	0.043
	V	1052 ± 29	0.11	51 ± 10(τ_{int})	0.029
GalNAc-6	I	841 ± 13	–	–	0.162
	II	846 ± 36	0.54	–	0.155
	III	–	–	315 ± 16	0.060
	IV	–	0.66	317 ± 10	0.043
	V	1052 ± 29	0.16	116 ± 14(τ_{int})	0.029

model-free approach to these data through a least-squares fitting procedure allowed one to estimate a global correlation time around 1100 ps (Table 8). Order parameters are higher for the Gal and Glc moieties (S^2 ca. 0.9) than for the Fuc and GalNAc residues (S^2 ca. 0.8). It can also be observed that there is a fairly good agreement between the experimentally deduced order parameters (Lipari and Szabo, 1982) and those estimated from the MD simulations. The data again indicate that all the rings display rather significant local motion, with fast correlation times around 100 ps. The fit of the carbon relaxation data to models I–IV was also performed. It can be observed that, at least for this particular case, the fitting is much better for the complete Lipari–Szabo (1982) spectral density function ($R_w = 0.029$) than for simplifications I–IV (R_w = 0.043–0.162). Thus, internal motions are contributing to relaxation parameters in an appreciable way. This is expected for internal reorientation timescales comparable to or shorter than the overall reorientation times. It is evident that some of the correlation times and order parameters deduced for the C-H vectors are different from those of the H-H pairs. This fact is not unexpected since both the motion and reorientation of both types of atom pairs are not necessarily the same. Finally, the analysis was also extended to the exocyclic C-6 carbon atoms (Table 9). It can be observed that the Glc hydroxymethyl group presents a higher restriction to motion than those of Gal and GalNAc as deduced from its higher order parameter. Again, the fit of the experimental data to the model-free approach V is much better than to models I–IV.

Regarding the nature of the motions deduced for this tetrasaccharide, the fast internal motion timescale (tens of picoseconds) is most probably related to librations of the pyranoid rings (Hajduk et al., 1993) and/or to reorientations around the glycosidic linkages (Lommerse et al., 1995). It has to be mentioned that the pyranoid rings are essentially monoconformational, as deduced from the vicinal proton–proton couplings. In any case, very slow motions related to chair interconversions (several tens of nanoseconds) would not significantly affect the form of the correlation function (Hajduk et al., 1993). Although the existence of other slow motions in the tetrasaccharide cannot be discarded, they can not be sampled within this framework. Internal motions contribute measurably to relaxation parameters, only if the corresponding internal reorientation timescales are comparable to or shorter than the overall reorientation times.

Molecular dynamics simulations

Information on the accessible conformational space for the glycosidic torsion angles of the tetrasaccharide was obtained through MD simulations in the presence of 545 explicit water molecules, using the CVFF force field (Hagler et al., 1979). This force field was used since it has provided satisfactory results in conformational studies of different oligosaccharide entities (Siebert et al., 1992; Asensio et al., 1995). Two different simulations of 200 ps each with explicit solvent, as well as one 1 ns in vacuo simulation were performed. Typical results are presented in Fig. 2. It can be observed that, although the glycosidic torsion angles do not flip between widely differing values,

they cover a substantial part of the complete Φ/Ψ map. Therefore, according to the simulations the torsional oscillations are constrained to a given area of the potential energy surface and no conformational transitions to other local minimum areas are observed. The average torsion angles for the different simulations are as follows: Gal/Glc, Φ/Ψ, 55/10; a range of oscillations of 45° and 35° were observed around these Φ and Ψ values, respectively. GalNAc/Gal, Φ/Ψ, –40/–25; oscillations of 60° and 100° were observed for Φ and Ψ, respectively. Fuc/Glc, Φ/Ψ, 50/25; oscillations of 60° and 35° were observed for Φ and Ψ, respectively. In order to characterize the time-scale and restriction to the internal motion around the glycosidic linkages, internal motion correlation functions were calculated for the different intra- and interresidue proton–proton (Fig. 3) and proton–carbon (Fig. 4) vectors of each of the residues of **1**, using a molecule-fixed coordinate frame, whereby global reorientation was removed (Bruschweiler et al., 1992; Abseher et al., 1994; Philippopoulos and Lim, 1994). It can be observed that, despite the short duration of the solvated simulations, the fast internal motions are satisfactorily sampled and the corresponding plateau is reached after a few picoseconds. These fast internal motions are most probably

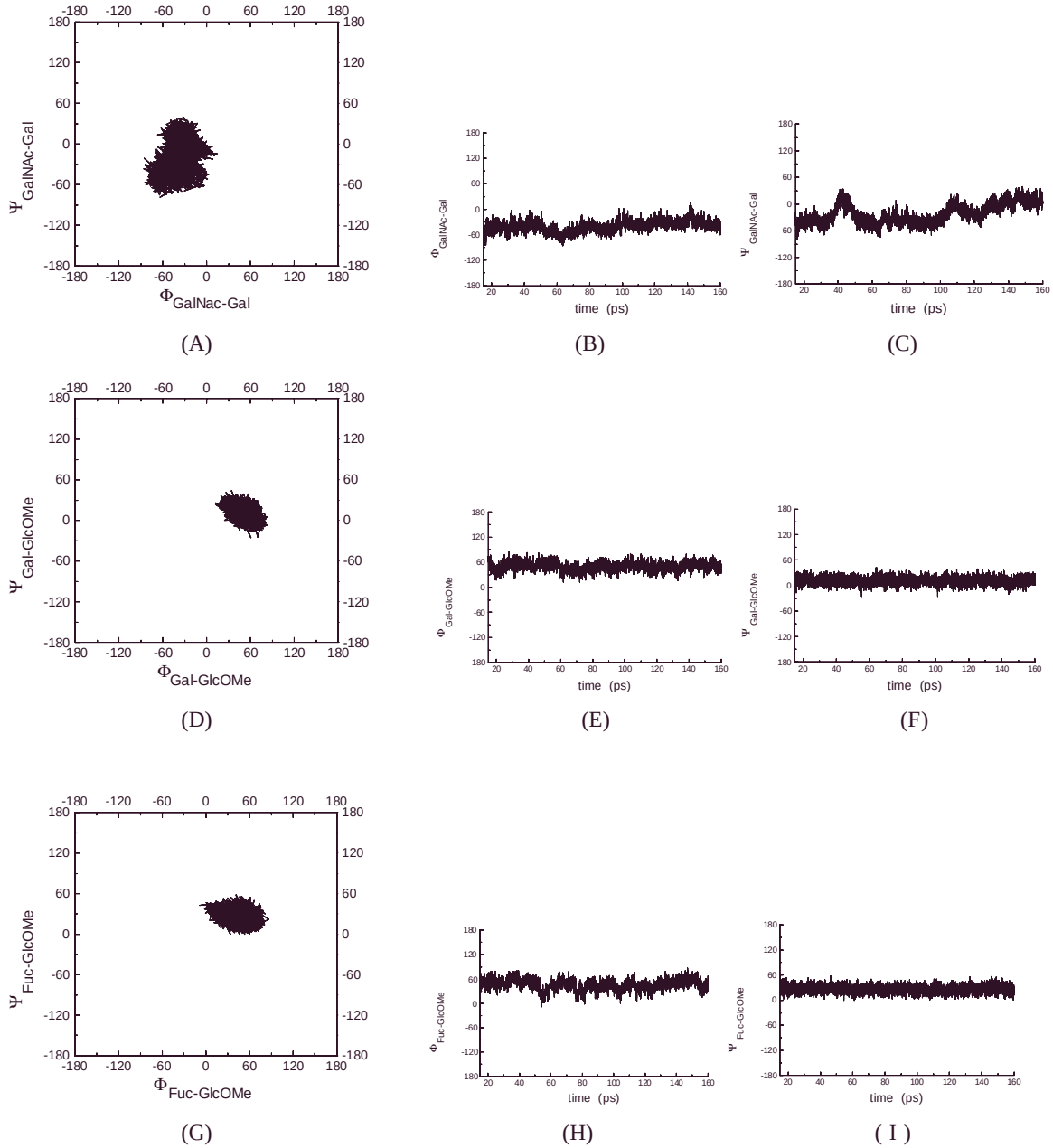

Fig. 2. History of Φ and Ψ angles during one MD simulation of **1** in a box of water molecules: (A) trajectory of the GalNAc/Gal linkage in Φ/Ψ space; (B) history of Φ; (C) history of Ψ; (D) trajectory of the Gal/Glc linkage in Φ/Ψ space; (E) history of Φ; (F) history of Ψ; (G) trajectory of the Fuc/Glc linkage in Φ/Ψ space; (H) history of Φ; (I) history of Ψ.

due to librations within a pyranoid ring (Hajduk et al., 1993) and/or motions within an energy well on the potential energy surface of the glycosidic linkages (Lommerse et al., 1995). The correlation functions were used to derive generalized order parameters and internal motion correlation times. These parameters were compared to those obtained from the experimental heteronuclear NMR relaxation measurements (see above). The calculated results from the solvated simulation again indicated a higher degree of restriction for the Glc and Gal residues (larger S^2), than for the GalNAc and Fuc moieties (smaller S^2), in agreement with the homo- and heteronuclear experimental data. In all cases, the internal correlation times around the glycosidic linkages were calcu-

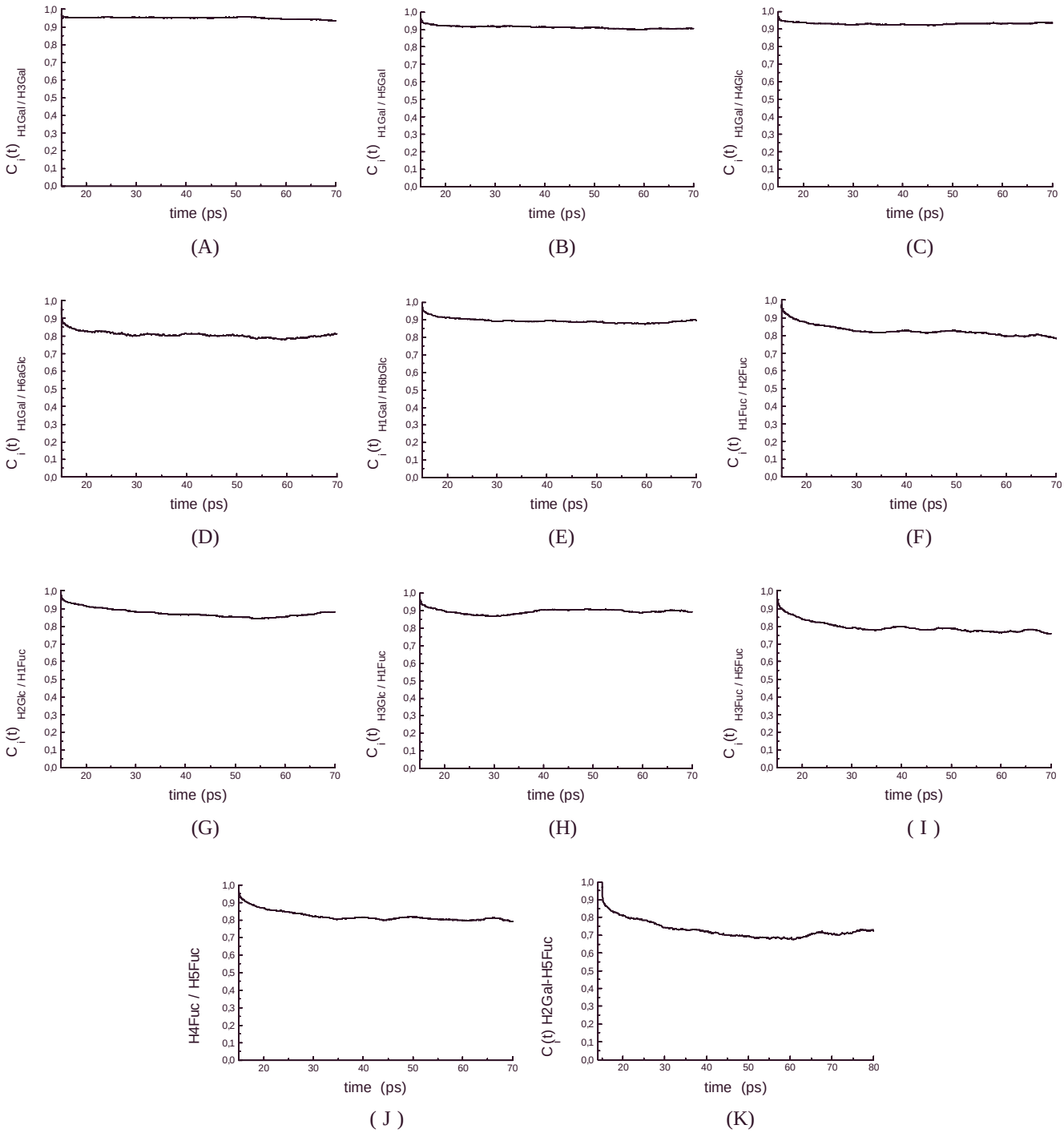

Fig. 3. Internal motion correlation functions for relevant intra- and interresidue proton pairs, calculated from the solvated MD simulation of **1**: (A) Gal H-1/Gal H-3; (B) Gal H-1/Gal H-5; (C) Gal H-1/Glc H-4; (D) Gal H-1/Glc H-6a; (E) Gal H-1/Glc H-6b; (F) Fuc H-1/Fuc H-2; (G) Fuc H-1/Glc H-2; (H) Fuc H-1/Glc H-3; (I) Fuc H-5/Fuc H-3; (J) Fuc H-5/Fuc H-4; (K) Fuc H-5/Gal H-2.

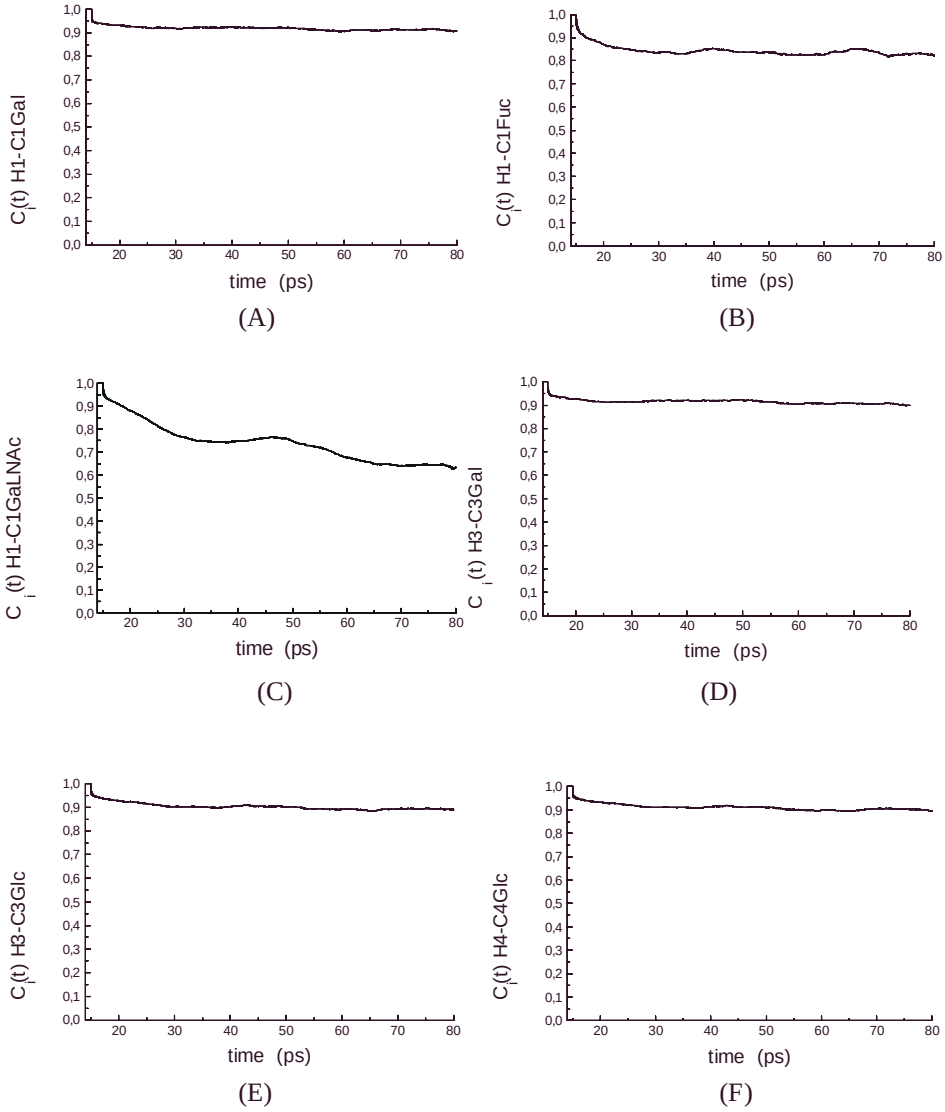

Fig. 4. Internal motion correlation functions for relevant C-H pairs, calculated from the solvated MD simulation of **1**: (A) Gal-1; (B) Fuc-1; (C) GalNAc-1; (D) Gal-3; (E) Glc-3; (F) Glc-4.

lated to be around a few tens of picoseconds. An in vacuo MD 1 ns simulation was also performed, which indicated an even higher degree of conformational freedom, with significantly smaller order parameters (between 0.15 and 0.30 units). Finally, average interproton distances were compared to those obtained from the experimental cross-relaxation rates (see above). It can be observed that there is a satisfactory agreement between both quantities. A superimposition of different conformers found in the solvated MD simulation is shown in Fig. 5. From an inspection of the major conformer, the relatively high order parameter deduced for Glc C-6 can be explained. The corresponding hydroxymethyl group is involved in van der Waals interactions with the vicinal galactose unit, in contrast to the observations for those of the Gal and GalNAc moieties which do not show additional interactions.

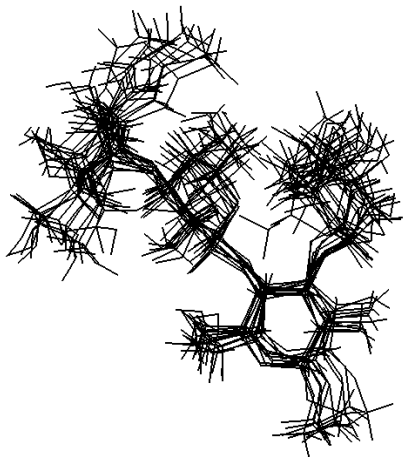

Fig. 5. Superimposition of the principal inertia axis of different snapshots taken during one of the solvated MD simulations of **1**, showing the flexibility of the different glycosidic linkages.

Conclusions

^{1}H-NMR data have shown that the glycosidic bonds of **1** in solution present distinct flexibility, in contrast with previously reported results for different analogues (Ball et al., 1992; Ichikawa et al., 1992). Nevertheless, it has to be mentioned that, very recently, an α-Fuc-(1→3)-GlcNAc glycosidic linkage within a glycopeptide (Lommerse et al., 1995) has also been shown to be rather flexible, in agreement with our observations. From a general point of view, it is shown that the recording of NOESY spectra at different temperatures may provide a direct and fast means to detect the presence of differential motions in oligosaccharides. The combined use of transversal and longitudinal cross-relaxation rates is sound and allows one to deduce the timescales and restrictions of motions affecting the spectral density functions. We have also shown, as also previously reported (Bagley et al., 1992; Roy et al., 1993; Dais, 1994; Kowalewski and Widmalm, 1994; Poppe et al., 1994; Engelsen et al., 1995; Maler et al., 1995,1996a,b), that, when experimentally accessible, the use of heteronuclear relaxation data, combined with the application of the model-free approach, does also account for the presence of internal motions in branched oligosaccharide molecules. Thus, the simultaneous use of homo- and heteronuclear relaxation NMR parameters, measured under different conditions and at several magnetic fields, provides different entries to detect molecular motions affecting dipolar relaxation in these biomolecules. CVFF molecular dynamics in a solvated system also produce estimates of order parameters, which, in this case, have been compared to experimental values (heteronuclear), providing a fairly satisfactory matching. The existence of flexibility for the Fuc moiety of **1**, and thus possibly for the closely related Le^X analogues, indicates that care should be taken when designing new substrates with potential therapeutic use, since the biologically active conformation may not be the major one existing in solution.

Acknowledgements

This work has been funded by DGICYT (PB-93-0127) and the Comunidad de Madrid (AE00049/95). We thank Prof. Martín-Lomas and Dr. Fernández-Mayoralas for their interest throughout this work. We also thank SIdI-UAM for support.

References

Abseher, R., Ludemann, S., Schreiber, H. and Steinhauser, O. (1994) *J. Am. Chem. Soc.*, **116**, 4006–4018.

Asensio, J.L., Martin-Pastor, M. and Jimenez-Barbero, J. (1995) *Int. J. Biol. Macromol.*, **17**, 52–55.

Bagley, S., Kovacs, H., Kowalewski, J. and Widmalm, G. (1992) *Magn. Reson. Chem.*, **30**, 733–739.

Ball, G.E., O'Neil, R.A., Schultz, J.E., Lowe, J.B., Weston, B.W., Nagy, J.O., Brown, E.G., Hobbs, C.J. and Bednarski, M.D. (1992) *J. Am. Chem. Soc.*, **114**, 5449–5451.

Barbato, G., Ikura, M., Kay, L.E., Pastor, R.W. and Bax, A. (1992) *Biochemistry*, **31**, 5269–5278.

Berthault, P., Birlirakis, N., Rubinstein, G., Sinäy, P. and Desvaux, H. (1996) *J. Biomol. NMR*, **8**, 23–35.

Bock, K. (1983) *Pure Appl. Chem.*, **55**, 605.

Bothner-By, A.A., Stephens, R.L., Lee, J.M., Warren, C.D. and Jeanloz, R.W. (1984) *J. Am. Chem. Soc.*, **106**, 811–813.

Braccini, I., Michon, V., Herve du Penhoat, C., Imberty, A. and Perez, S. (1993) *Int. J. Biol. Macromol.*, **15**, 52–55.

Bruschweiler, R., Roux, B., Blackledge, M., Griesinger, C., Karplus, M. and Ernst, R.R. (1992) *J. Am. Chem. Soc.*, **114**, 2289–2302.

Bundle, D.R. and Young, N.M. (1992) *Curr. Opin. Struct. Biol.*, **2**, 666.

Bush, C.A. (1992) *Curr. Opin. Struct. Biol.*, **2**, 655–663.

Carver, J.P. (1993) *Pure Appl. Chem.*, **65**, 763.

Coteron, J.M., Singh, K., Asensio, J.L., Dalda, M.D., Fernández-Mayoralas, A., Jiménez-Barbero, J. and Martín-Lomas, M. (1995) *J. Org. Chem.*, **60**, 1502.

Craik, D.J., Kumar, A. and Levy, G.C. (1983) *Chem. Inf. Comput. Chem.*, **23**, 30.

Dabrowski, J., Kozar, T., Grosskurth, H. and Nifant'ev, N.E. (1995) *J. Am. Chem. Soc.*, **117**, 5534.

Dais, P. (1994) *Carbohydr. Res.*, **263**, 13–24.

Davis, D.G. (1987) *J. Am. Chem. Soc.*, **109**, 3471–3472.

De Waard, P., Leeflang, B.R., Vliegenthart, J.F.G., Boelens, R., Vuister, G. and Kaptein, R. (1992) *J. Biomol. NMR*, **2**, 211–226.

Edge, C.J., Singh, U.C., Bazzo, R., Taylor, G.L., Dwek, R.A. and Rademacher, T.W. (1990) *Biochemistry*, **29**, 1971–1974.

Ejchart, A., Dabrowski, J. and Von der Lieth, C.-W. (1992) *Magn. Reson. Chem.*, **30**, 105–S114.

Ejchart, A. and Dabrowski, J. (1992) *Magn. Reson. Chem.*, **30**, 115–S124.

Engelsen, S.B., Herve du Penhoat, C. and Perez, S. (1995) *J. Phys. Chem.*, **99**, 13334–13351.

Gonzalez, C., Rullman, J.A.C., Boelens, R. and Kaptein, R. (1991) *J. Magn. Reson.*, **91**, 659–664.

Hagler, A.T., Lifson, S. and Dauber, P. (1979) *J. Am. Chem. Soc.*, **101**, 5122–5130.

Hajduk, P.J., Horita, D.A. and Lerner, L. (1993) *J. Am. Chem. Soc.*, **115**, 9196–9201.

Hardy, B.J., Egan, W. and Widmalm, G. (1995) *Int. J. Biol. Macromol.*, **17**–**18**, 149–160.

Homans, S.W. (1990) *Prog. NMR Spectrosc.*, **22**, 55.

Homans, S.W. and Forster, M. (1992) *Glycobiology*, **2**, 143–151.

Hricovini, M., Shah, R.N. and Carver, J.P. (1992) *Biochemistry*, **31**, 10018–10023.

Hricovini, M. and Torri, G. (1995) *Carbohydr. Res.*, **268**, 159–175.

Ichikawa, Y., Lin, Y.C., Dumas, D.P., Shen, G.-J., Garcia-Junceda, E., Williams, M.A., Bayer, R., Ketcham, C., Walker, L.E., Paulson, J.C. and Wong, C.-H. (1992) *J. Am. Chem. Soc.*, **114**, 9283.

Kay, L.E., Nicholson, L.K., Delaglio, F., Bax, A., Torchia, D. (1992) *J. Magn. Reson.*, **97**, 359–375.

Kowalewski, J. and Widmalm, G. (1994) *J. Phys. Chem.*, **98**, 28–34.

Lasky, L.A. (1992) *Science*, **258**, 964.

Leeflang, B.R. and Kroon-Batenburg, L.M.J. (1992) *J. Biomol. NMR*, **2**, 495–518.

Lemieux, R.U., Bock, K., Delbaere, L.T.J., Koto, S. and Rao, V.S. (1980) *Can. J. Chem.*, **58**, 631–653.

Lemieux, R.U. (1989) *Chem. Soc. Rev.*, **18**, 347.

Lipari, G. and Szabo, A. (1982) *J. Am. Chem. Soc.*, **104**, 4546–4559.

Lommerse, J.P.M., Kroon-Batenburg, L.M.J., Kroon, J., Kamerling, J.P. and Vliegenthart, J.F.G. (1995) *J. Biomol. NMR*, **6**, 79–94.

Maler, L., Lang, J., Widmalm, G. and Kowalewski, J. (1995) *Magn. Reson. Chem.*, **33**, 541–548.

Maler, L., Widmalm, G. and Kowalewski, J. (1996a) *J. Biomol. NMR*, **7**, 1–7.

Maler, L., Widmalm, G. and Kowalewski, J. (1996b) *J. Phys. Chem.*, **100**, 17103–17110.

Meyer, C., Perez, S., Herve du Penhoat, C. and Michon, V. (1993) *J. Am. Chem. Soc.*, **115**, 10300.

Mukhopadhyay, C., Miller, K.E. and Bush, C.A. (1994) *Biopolymers*, **34**, 21.

Neuhaus, D. and Williamson, M.P. (Eds.) (1989) *The Nuclear Overhauser Effect in Structural and Conformational Analysis*, VCH, New York, NY, U.S.A.

Peters, T., Meyer, B., Stuike-Prill, R., Somorjai, R. and Brisson, J.-R. (1993) *Carbohydr. Res.*, **238**, 49.

Peters, T. and Weimar, T. (1994) *J. Biomol. NMR*, **4**, 97–116.

Philippopoulos, M. and Lim, C. (1994) *J. Phys. Chem.*, **98**, 8264–8273.

Poppe, L. and Van Halbeek, H. (1992) *J. Am. Chem. Soc.*, **114**, 1092–1093.

Poppe, L., Van Halbeek, H., Acquotti, D. and Sonnino, S. (1994) *Biophys. J.*, **66**, 1642–1652.

Poveda, A., Asensio, J.L., Martín-Pastor, M. and Jiménez-Barbero, J. (1996) *Chem. Commun.*, 421–422.

Rice, K.G., Wu, P., Brand, L. and Lee, Y.C. (1993) *Curr. Opin. Struct. Biol.*, **3**, 669–674.

Roy, R., Tropper, F.D., Williams, A.J. and Brisson, J.R. (1993) *Can. J. Chem.*, **71**, 1995–2006.

Rutherford, T.J., Partridge, J., Weller, C.T. and Homans, S.W. (1993) *Biochemistry*, **32**, 12715.

Rutherford, T.J. and Homans, S.W. (1994) *Biochemistry*, **33**, 9606–9614.

Rutherford, T.J., Spackman, D.G., Simpson, P.J. and Homans, S.W. (1994) *Glycobiology*, **4**, 59.

Rutherford, T.J., Neville, D.C.A. and Homans, S.W. (1995) *Biochemistry*, **34**, 14131–14137.

Santos-Benito, F.F., Fernández-Mayoralas, A., Martín-Lomas, M. and Nieto-Sampedro, M. (1992) *J. Exp. Med.*, **176**, 915.

Searle, M.S. and Williams, D.H. (1992) *J. Am. Chem. Soc.*, **114**, 10690.

Siebert, H.-C., Reuter, G., Schauer, R., Von der Lieth, C.-W. and Dabrowski, J. (1992) *Biochemistry*, **31**, 6962–6971.

Singh, K., Fernández-Mayoralas, A. and Martín-Lomas, M. (1994) *J. Chem. Soc., Chem. Commun.*, 775.

Van Halbeek, H. and Poppe, L. (1992) *Magn. Reson. Chem.*, **30**, 74–S86.

Van Halbeek, H. (1994) *Curr. Opin. Struct. Biol.*, **4**, 697–709.

Wagner, G. (1993) *Curr. Opin. Struct. Biol.*, **3**, 748–754.

Yan, Z.-Y., Rao, B.N.N. and Bush, C.A. (1987) *J. Am. Chem. Soc.*, **109**, 7663–7669.